Observations of M33 H II Regions: the Ne/S ratio, metallicity, and ionization variations

Robert H. Rubin[1,2], Janet P. Simpson[1,3], Ian A. McNabb[1], Gregory Brunner[4], Sean W.J. Colgan[1], Reginald J. Dufour[4], Adalbert W.A. Pauldrach[5], Alex D. Browne[1], Robert Zhang[1], and Eric J. Csongradi[1]

ABSTRACT

We have observed emission lines of [S IV] 10.51, H(7–6) 12.37, [Ne II] 12.81, [Ne III] 15.56, and [S III] 18.71 μm in a number of extragalactic H II regions with the *Spitzer Space Telescope*. A previous paper presented our data and analysis for the substantially face-on spiral galaxy M83. Here we report our results for the local group spiral galaxy M33. The nebulae selected cover a wide range of galactocentric radii (R_G). The observations were made with the Infrared Spectrograph with the short wavelength, high resolution module. The above set of five lines is observed cospatially, thus permitting a reliable comparison of the fluxes. From the measured fluxes, we determine the ionic abundance ratios including Ne^{++}/Ne^{+}, S^{3+}/S^{++}, and S^{++}/Ne^{+} and find that there is a correlation of increasingly higher ionization with larger R_G. By sampling the dominant ionization states of Ne (Ne^{+}, Ne^{++}) and S (S^{++}, S^{3+}) for H II regions, we can estimate the Ne/H, S/H, and Ne/S ratios. We find that there is a decrease in metallicity with increasing R_G. There is no apparent variation in the Ne/S ratio with R_G. Unlike our previous similar study of M83, where we conjectured that this ratio was an upper limit, for M33 the derived ratios are likely a robust indication of Ne/S. This occurs because the H II regions have lower metallicity and higher ionization than those in M83. Both Ne and S are primary elements produced in α-chain reactions, following C and O burning in stars, making their yields depend very little on the stellar metallicity. Thus, it is expected that Ne/S remains relatively constant throughout a galaxy. The median (average) Ne/S ratio

[1]NASA/Ames Research Center, Moffett Field, CA 94035-1000, USA

[2]Orion Enterprises, M.S. 245-6, Moffett Field, CA 94035-1000, USA

[3]SETI Institute, 515 N. Whisman Road, Mountain View, CA 94043, USA

[4]Physics & Astronomy Department, Rice University, MS 61, Houston, TX 77005-1892, USA

[5]University of Munich, Munich D-81679, Germany

derived for H II regions in M33 is 16.3 (16.9), just slightly higher than the Orion Nebula value of 14.3. These values are in sharp contrast with the much lower "canonical", but controversial, solar value of ∼5. A recent nucleosynthesis, galactic chemical evolution model predicts a Ne/S abundance of ∼9. Our observations may also be used to test the predicted ionizing spectral energy distribution of various stellar atmosphere models. We compare the ratio of fractional ionizations $<Ne^{++}>/<S^{++}>$, $<Ne^{++}>/<S^{3+}>$, and $<Ne^{++}>/<Ne^{+}>$ vs. $<S^{3+}>/<S^{++}>$ with predictions made from our photoionization models using several of the state-of-the-art stellar atmosphere model grids. The trends of the ionic ratios established from the prior M83 study are remarkably similar, but continued to higher ionization with the present M33 objects.

Subject headings: ISM: abundances, H II regions, stars: atmospheres, galaxies: individual (M33)

1. *Spitzer Space Telescope* Observations

Most of the observations were made in 2006, January 15 to February 1 (UT) during *SST*/IRS campaign 28. The last set of observations, one Astronomical Observing Request (AOR) out of a total of 8, was made on 2007, February 11 during *SST*/IRS campaign 38. Table 1 lists the H II region positions and the aperture grid configuration used to observe each. The nebulae are designated by their BCLMP number (Boulesteix et al. 1974). The H II regions observed in the remaining AOR in 2007 were #62, 302, 691, 651, and 740W. The size of the SH aperture is $11.3'' \times 4.7''$. Maps were arranged with the apertures overlapping along the direction of the long slit axis ("parallel" direction). The purpose of overlapping is that most spatial positions will be covered in at least two locations on the array, minimizing the effects of bad detectors. In the direction of the short slit axis ("perpendicular" direction), the apertures were arranged abutting each other with no overlap or space between them. In all cases, we chose the mapping mode with aperture grid patterns varying from a 1×2 grid to as large as a 2×4 grid in order to cover the bulk of the expected emission.

The emission lines were measured with SMART using a Gaussian line fit. The continuum baseline was fit with a linear or quadratic function. Figures 1 (a) & (b) show the fits for two lines in BCLMP 45. A line is deemed to be detected if the flux is at least as large as the 3 σ uncertainty. We measure the uncertainty by the product of the full-width-half-maximum (FWHM) and the root-mean-square variations in the adjacent, line-free continuum; it does not include systematic effects. For the brighter lines, that is, most of the 10.5, 12.8, 15.6, and 18.7 μm lines, the systematic uncertainty far exceeds the measured (statistical) uncertainty.

Table 1. H II Regions Observed in M33

Order	H II Region	RA	J2000 DEC	Aperture Grid	Order	H II Region	RA	J2000 DEC	Aperture Grid
1	280	1 32 45.4	30 38 56	2x4	14	301	1 33 55.6	30 45 27	1x3
2	230	1 33 00.7	30 34 17	1x3	15	4	1 33 59.3	30 35 48	1x3
3	277	1 33 12.2	30 38 49	2x3	16	79	1 34 00.2	30 40 51	1x3
4	638	1 33 16.0	30 56 45	2x3	17	87E	1 34 02.3	30 38 45	1x3
5	623	1 33 16.4	30 52 47	1x3	18	302	1 34 06.9	30 47 27	1x3
6	45	1 33 29.2	30 40 25	2x3	19	702	1 34 10.2	30 31 54	1x2
7	214	1 33 30.0	30 31 47	1x3	20	95	1 34 11.2	30 36 16	1x3
8	33	1 33 34.9	30 37 06	1x3	21	710	1 34 13.8	30 33 44	1x3
9	42	1 33 35.6	30 39 30	1x2	22	88W	1 34 15.3	30 37 11	1x3
10	32	1 33 35.8	30 36 29	1x3	23	691	1 34 16.5	30 51 56	1x3
11	251	1 33 36.7	30 20 13	1x3	24	651	1 34 29.8	30 57 15	1x3
12	62	1 33 44.7	30 44 38	1x3	25	740W	1 34 39.8	30 41 54	1x3
13	27	1 33 46.1	30 36 54	1x2					

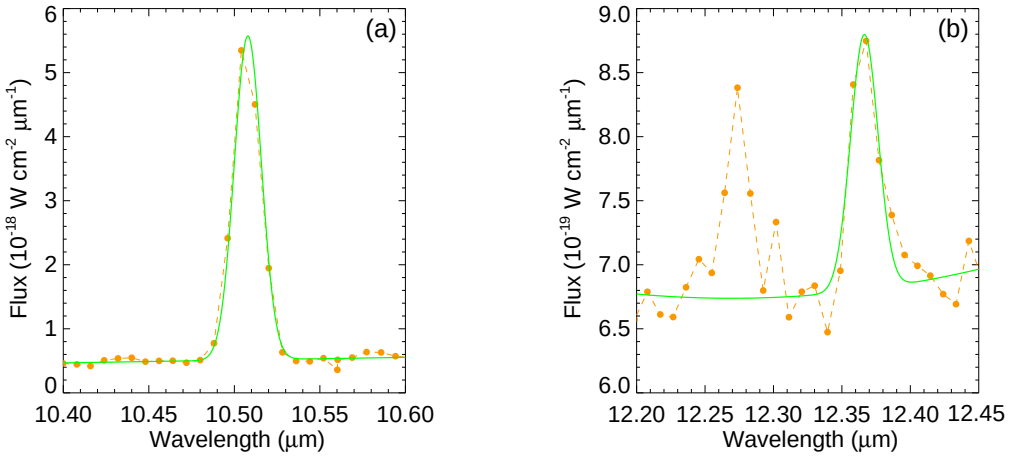

Fig. 1.— Measurements of two of the five emission lines in the H II region BCLMP 45: **(a)** [S IV] 10.5 μm and **(b)** H(7–6) 12.4 μm; the feature on the blue side is H_2 S(2). The data points are the filled circles. The fits to the continuum and Gaussian profiles are the solid lines. Such measurements provide the set of line fluxes for further analysis.

Even for the fainter lines, we estimate that the systematic uncertainty exceeds the measured uncertainty. In addition to the line flux, the measured FWHM and heliocentric radial velocities (V_{helio}) can be found in Table 2 of Rubin et al. (2008, henceforth R08).

2. Variation in the metallicity and ionization of the H II regions with R_G

We present the variation of Ne^{++}/Ne^{+} with R_G in Figure 2(a) using the values from Table 3 (in R08). The error values represent the propagated flux measurement uncertainties and do not include the systematic uncertainties. A linear and logarithmic least-squares fit indicates a positive correlation with R_G (in kpc),

$$Ne^{++}/Ne^{+} = -0.44\pm0.22 + (0.46\pm0.067)\ R_G, \text{ and}$$

$$\log(Ne^{++}/Ne^{+}) = -0.88\pm0.11 + (0.20\pm0.035)\ R_G.$$

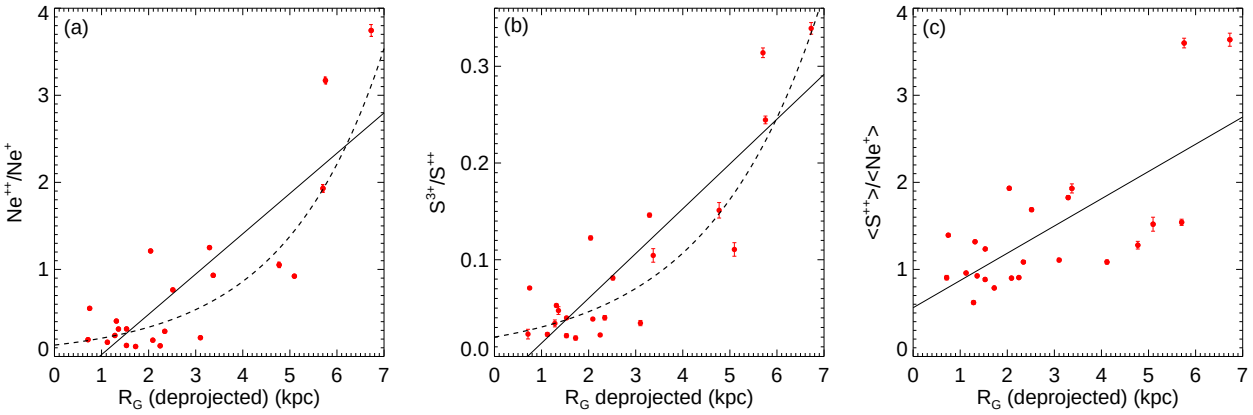

Fig. 2.— Plots of ionic abundance ratios of H II regions in M33 with R_G: **(a)** Ne^{++}/Ne^{+} vs. R_G, **(b)** S^{3+}/S^{++} vs. R_G, and **(c)** $<S^{++}>/<Ne^{+}>$ vs. R_G.

For all the least-squares line fits in this paper, each point is given equal weight because systematic uncertainties exceed the flux measurement uncertainties, as discussed earlier. The positive correlation of Ne^{++}/Ne^{+} with R_G as measured by the slope may be judged to be significant following the criterion that it exceeds the 3 σ uncertainty. The transformation of this function is shown as the dashed line in Figure 2(a). The slope in the linear plot here 0.46±0.067 is much steeper than the analogous slope for our M83 H II regions of 0.011±0.0035 (see Figure 3 in Rubin et al. 2007, henceforth R07). Furthermore, the comparison with Figure 3 in the M83 paper shows dramatically the higher ionization of the M33 nebulae.

A similar fit to the linear and log relations of the S^{3+}/S^{++} vs. R_G data yields

$$S^{3+}/S^{++} = -0.032\pm0.018 + (0.046\pm0.0057)\ R_G, \text{ and}$$

$$\log(S^{3+}/S^{++}) = -1.7\pm0.090 + (0.18\pm0.028)\ R_G.$$

The slope in both fits is also statistically significant. We map the logarithmic relation onto Figure 2(b) as the dashed line. While there is no fundamental reason to expect either functional form shown in Figures 2(a) & (b), we note that the dashed line fits do have the advantage of not extrapolating to negative ionic ratios at small values of R_G.

Figure 2(c) plots the fractional ionic abundance ratio $<S^{++}>/<Ne^{+}>$ vs. R_G. This ratio is obtained from the S^{++}/Ne^{+} ratio by multiplying by an assumed Ne/S value (see below). Table 3 (in R08) lists this and other fractional ionic abundance ratios used in this paper. We show the linear least-squares fit for an assumed N_e of 100 cm^{-3}. Here, the fit indicates a significant positive correlation with R_G,

$$<S^{++}>/<Ne^{+}> = 0.56\pm0.23 + (0.31\pm0.069)\ R_G,$$

where angular brackets denote fractional ionization. In this figure and in the linear fit, we assume an Orion Nebula Ne/S abundance ratio of 14.3 (Simpson et al. 2004). Because Ne

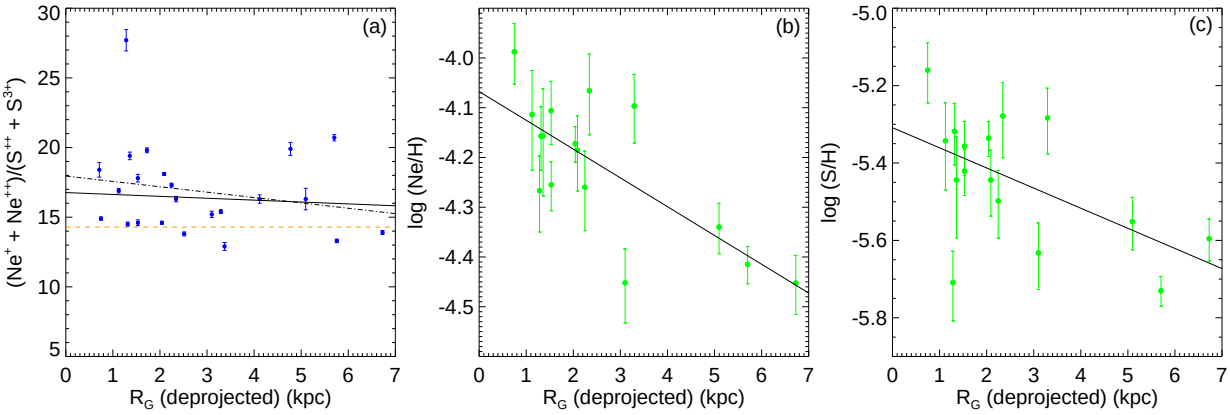

Fig. 3.— **(a)** Ne/S, as approximated by $(Ne^+ + Ne^{++})/(S^{++} + S^{3+})$, vs. R_G, **(b)** log (Ne/H) vs. R_G, and **(c)** log (S/H) vs. R_G.

and S are "primary" elements, their production is expected to vary in lockstep and Ne/S would not be expected to show a radial gradient within a galaxy. There is a clear correlation of increasingly higher ionization with increasing R_G.

For H II regions, we may approximate the Ne/S ratio with $(Ne^+ + Ne^{++})/(S^{++} + S^{3+})$. This includes the dominant ionization states of these two elements. However this relation does not account for S^+, which should be present at some level. We may safely ignore the negligible contributions of neutral Ne and S in the ionized region. Figure 3(a) shows our approximation for Ne/S vs. R_G with the relation

$$\mathrm{Ne/S} = 16.8\pm0.97 - (0.14\pm0.29)\ R_G.$$

This is a fit to 22 objects while the steeper dot-dash line includes the most deviant large value (source 32). Both fits indicate that there is no significant slope. Our data also indicate that the lower envelope to Ne/S is well fit by a constant value equal to the Orion Nebula ratio of 14.3 (Simpson et al. 2004).

There was a significant detection of the H(7-6) flux for 16 of the H II regions (see Table 2 in R08) which permits a determination of the heavy element abundances Ne/H and S/H (see Table 3 in R08). We present the results for Ne/H in Figure 3(b). A linear least-squares fit of log (Ne/H) vs. R_G results in

$$\log\ (\mathrm{Ne/H}) = -4.07\pm0.04 - (0.058\pm0.014)\ R_G.$$

This fit indicates a significant slope. A similar plot for S/H is shown in Figure 3(c). Here the linear least-squares fit to log (S/H) vs. R_G yields

$$\log\ (\mathrm{S/H}) = -5.31\pm0.06 - (0.052\pm0.021)\ R_G.$$

It is interesting that the slope is nearly identical to the Ne/H relationship. However, the

slope is deemed only marginally significant. While *Spitzer* is an admirable machine for measuring both Ne and S abundances in H II regions, the neon abundances are determined more reliably. As previously mentioned, with the *Spitzer* observations alone, we are neither accounting for S^+ nor S that may be tied up in dust or molecules. In this sense, the S/H ratios in Figure 3(c) are lower limits. Both of the above measurements of a heavy element abundance gradient are in remarkable agreement with the recent value for the log (O/H) gradient of -0.054 ± 0.011 dex kpc^{-1} (Magrini et al. 2007). They derived this gradient from optical observations of 14 H II regions in M33 where a value for T_e was determined.

3. Constraints on the ionizing SED for the stars exciting the H II regions

In Figures 4(a), (b), and (c), we plot respectively the ratio of fractional ionizations $<Ne^{++}>/<S^{++}>$, $<Ne^{++}>/<S^{3+}>$, and $<Ne^{++}>/<Ne^{+}>$ vs. $<S^{3+}>/<S^{++}>$. These ionic ratios are computed using our photoionization code NEBULA (e.g., Simpson et al. 2004; Rodríguez & Rubin 2005). The lines connect the results of the nebular models calculated using the ionizing SEDs predicted from various stellar atmosphere models. There are no other changes to the input parameters, just the SED. The stellar atmospheres used are representative of several non-LTE models that apply for O-stars. We also display the results from one set of LTE models (Kurucz 1992). Figures 4(a)–(c) dramatically illustrate how sensitive H II region model predictions of these ionic abundance ratios are to the ionizing SED input to nebular plasma simulations. The open red circles are our prior results for the M83 H II regions. The green stars are the M33 results derived from our observed line fluxes also using N_e of 100 cm^{-3} and adjusting by the assumed Ne/S. While the $<Ne^{++}>/<Ne^{+}>$ ratio in Figure 4(c) has the advantage of being independent of elemental abundance ratios, it appears to be more sensitive to the *nebular* parameters than the others (R08). The trends of the ionic ratios established from the prior M83 study are remarkably similar, but continued to higher ionization with the present M33 objects. On the whole, the data for both galaxies in panels (a) and (b) lie closest to the theoretical loci obtained with the Pauldrach et al. supergiant SEDs. This is particularly notable in Figure 4(b), where the other model loci are nearly perpendicular to the data point trend in the vicinity of where they intersect the data points. On the other hand, the data in panel (c), for the most part, appear to lie closer to Martins et al., Lanz & Hubeny et al., and Pauldrach et al. *dwarf* locus. The nebular models used to generate Figures 4 are all constant density, ionization-bounded, spherical models. We used a constant total nucleon density (DENS) of 1000 cm^{-3} that begins at the star. Each model used a total number of Lyman continuum photons s^{-1} (N_{Lyc}) = 10^{49}. The same *nebular* elemental abundance set was used for all nebular models (R08).

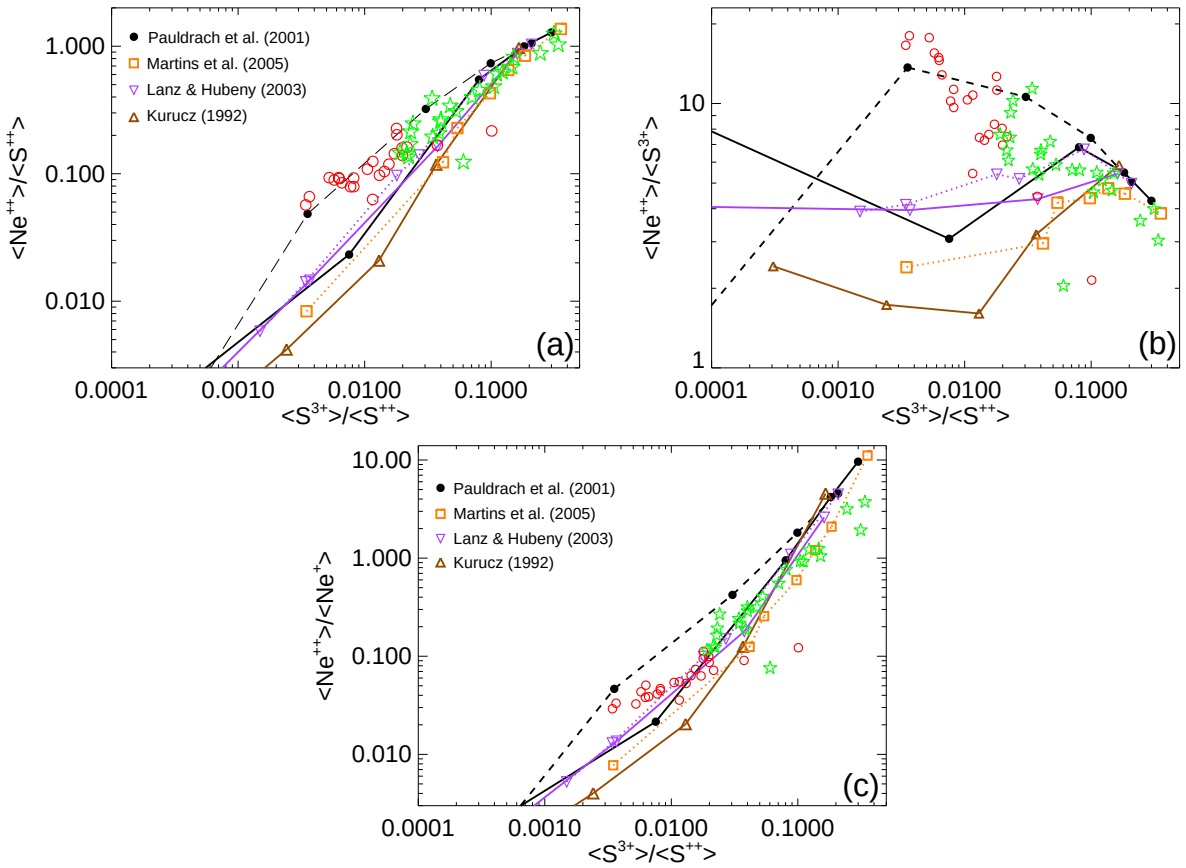

Fig. 4. — **(a)** Theoretical predictions of the fractional ionization ratios $<Ne^{++}>/<S^{++}>$ vs. $<S^{3+}>/<S^{++}>$, computed using our photoionization code NEBULA. The lines connect the results of nebular models calculated with the ionizing SEDs predicted from various stellar atmosphere models as labeled, changing no other parameter except the SED. For the H II region models calculated with Pauldrach et al. atmospheres, the solid line connects models with dwarf atmospheres and the dashed line connects models with supergiant atmospheres. The violet loci join models calculated with Lanz & Hubeny atmospheres: solid line with log g= 4.0 and the dotted line a set with smaller log g. The dotted orange line connects models using Martins et al. atmospheres. The brown line presents results using Kurucz atmospheres. To compare our data with the models in Figures 4(a) & (b), we need to divide the observed Ne^{++}/S^{++} and Ne^{++}/S^{3+} ratios by an assumed Ne/S abundance ratio. We use the Orion Nebula Ne/S = 14.3. The open red circles are our prior results for the M83 H II regions. The green stars are the M33 results derived from our observed line fluxes using N_e of 100 cm^{-3}.
(b) The same as panel (a) except the ordinate is $<Ne^{++}>/<S^{3+}>$. These data, for the most part, appear to track the Pauldrach et al. supergiant locus.
(c) Similar to panels (a) and (b) except the ordinate is $<Ne^{++}>/<Ne^{+}>$. These data, for the most part, appear to lie closer to Martins et al., Lanz & Hubeny et al., and Pauldrach et al. *dwarf* loci.

4. Discussion

The data presented here for M33, combined with other *Spitzer* data (see Figures 11 and 12 in R08), are consistent with our view that there are now reliable estimates for the *total* Ne/S ratio. As long as the degree of ionization is sufficiently high such that the amount of sulfur in forms other than S^{++} and S^{3+} is small, the methodology used here will provide a robust total Ne/S estimate. The median Ne/S value we derive for the M33 objects is 16.3, but this includes many with relatively low ionization.

The solar abundance, particularly of Ne, remains the subject of much controversy (e.g., Drake & Testa 2005; Bahcall, Serenelli, & Basu 2006). While we cannot directly address the solar abundance with our observations of extragalactic H II regions, it is important to have reliable benchmarks for the Ne abundance. There appears to be a growing body of evidence that the Ne abundance [its fractional number abundance relative to H log H = 12, by definition and termed A(H)] is substantially higher in the solar neighborhood, and even in the Sun itself, than the "canonical" solar values given in two often-referenced papers. These papers have for the Sun: A(Ne) = 7.87, A(S) = 7.19 (Lodders 2003) and A(Ne) = 7.84, A(S) = 7.14 (Asplund, Grevesse, & Sauval 2005). Thus according to both, Ne/S ∼5. It is now generally accepted that Ne has the least well determined solar abundance among the most abundant elements. One of the proponents for a higher neon abundance pointed out that an A(Ne) = 8.29 would reconcile solar models with the helioseismological measurements (Bahcall, Basu, & Serenelli 2005). Using this value together with the A(S) values above, we obtain Ne/S of 12.6 and 14.1, respectively, close to the Orion Nebula ratio 14.3 and the various median ratios that range from 10.1 to 16.3 (R08).

In our earlier M83 paper (R07), we discussed what the Ne/S ratio was predicted to be according to calculations based on the theoretical nucleosynthesis, galactic chemical evolution models of Timmes, Woosley, & Weaver (1995). The ratio was about 3.8. Since then there have been improved models (Woosley & Heger 2007). Based on Fig. 7 in Woosley & Heger (2007), the Ne/S ratio is predicted to be ∼8.6.

This work is based on observations made with the *Spitzer Space Telescope* , which is operated by the Jet Propulsion Laboratory, California Institute of Technology under NASA contract 1407. Support for this work was provided by NASA for this *Spitzer* program identification 20057. We thank Stan Woosley for providing information on the Ne/S ratio from a nucleosynthesis, galactic chemical evolution perspective. We thank Danny Key, Erik Krasner-Karpen, and Matt Lattanzi for assistance with the data reduction. The nebular models were run on JPL computers. Funding for their use was provided by the JPL Office of the Chief Information Officer.

REFERENCES

Asplund, M., Grevesse, N., & Sauval, A.J. 2005, in Cosmic Abundances as Records of Stellar Evolution & Nucleosynthesis, ed. T.G. Barnes III, F.N. Bash, ASP Conf., 336, 25

Bahcall, J.N, Basu, S., & Serenelli, A.M. 2005, ApJ, 631, 1281

Bahcall, J.N., Serenelli, A.M., & Basu, S. 2006, ApJS, 165, 400

Boulesteix, J., Courtès, G., Laval, A., Monnet, G., & Petit, H. 1974, A&A, 37, 33

Corbelli, E., & Schneider, S.E. 1997, ApJ, 479, 244

Drake, J.J., & Testa, P. 2005, Nature, 436, 525

Kurucz, R.L. 1992, in IAU Symp. 149, Stellar Population of Galaxies, p. 225

Lanz, T., & Hubeny, I. 2003, ApJS, 146, 417

Lodders, K. 2003, ApJ, 591, 1220

Magrini, L., Vílchez, J.M., Mampaso, A., Corradi, R.L.M., & Leisy, P. 2007, A&A, 470, 865

Martins, F., Schaerer, D., & Hillier, D.J. 2005, A&A, 436, 1049

Pauldrach, A.W.A., Hoffmann, T.L., & Lennon M. 2001, A&A, 375, 161

Rodríguez, M., & Rubin, R.H. 2005, ApJ, 626, 900

Rubin, R.H., Simpson, J.P., Colgan, S.W.J., Dufour, R.J., Ray, K.L., Erickson, E.F., Haas, M.R., Pauldrach, A.W.A., & Citron, R.I. 2007, MNRAS, 377, 1407 (R07)

Rubin, R.H., Simpson, J.P., Colgan, S.W.J., Dufour, R.J., Brunner, G., McNabb, I.A., Pauldrach, A.W.A., Erickson, E.F., Haas, M.R., & Citron R.I. 2008, MNRAS, (submitted) (R08)

Simpson, J.P., Rubin, R.H., Colgan, S.W.J., Erickson, E.F., & Haas, M.R. 2004, ApJ, 611, 338

Timmes, F.X., Woosley, S.E., & Weaver, T.A. 1995, ApJS, 98, 617

Woosley, S.E., & Heger, A. 2007, PhR, 442, 269